

# Managing Complications of Interventional Oncology Procedures

A compilation of cases demonstrating complications that may be encountered during oncologic procedures of the liver, kidney, and lung and their management.

## Introduction

By Siddharth A. Padia, MD

Interventional oncology (IO) plays a pivotal role in many solid organ malignancies. Ablation or embolization is the standard of care for many renal and hepatic cancers, and both have played an increasing role in the treatment of pulmonary neoplasms. Although most outcomes of locoregional therapy are based on tumor response and prolongation of survival, the successful growth of IO is partly due to a very low rate of significant adverse events. Major complications from minimally invasive oncologic interventions continue to be rare, despite the advent of new techniques over the past several years. This article uses a case-based format to present

five complications from oncologic procedures of the liver, kidney, and lung. Knowledge of these adverse events and strategies for treatment are outlined.

### Siddharth A. Padia, MD

Section of Interventional Radiology  
Department of Radiology  
David Geffen School of Medicine  
University of California Los Angeles  
Los Angeles, California  
spadia@mednet.ucla.edu

*Disclosures: Consultant for Boston Scientific Corporation, Teleflex Medical, Guerbet, and Varian Medical Systems.*

## Complete Response of Large HCC After Acute Ascending Aortic Dissection Following Portal Vein Embolization and Concurrent Immunotherapy

By Cynthia De la Garza-Ramos, MD; Beau B. Toskich, MD; and Andrew R. Lewis, MD

Surgical resection is the preferred treatment for patients with hepatocellular carcinoma (HCC) and Child-Pugh class A liver disease without portal hypertension.<sup>1</sup> Perioperative assessment for resection takes into consideration tumor and patient factors, as well as the future liver remnant (FLR). Radiation lobectomy with yttrium-90 (Y-90) and portal vein embolization (PVE) can be used to increase resection candidacy by inducing

contralateral lobe hypertrophy.<sup>2</sup> Radiation lobectomy provides tumoricidal effects and, despite slower hepatic volume changes than PVE, may provide assurance against posthepatectomy liver failure by ablating the future resection site (FRS).<sup>3,4</sup> Alternatively, PVE induces more rapid volumetric changes than radiation lobectomy, allowing a shorter time to resection, but does not ablate the primary tumor or FRS. Both radiation lobectomy and

PVE are useful as part of a multidisciplinary hepatobiliary program and are not mutually exclusive.

## CASE STUDY

### Initial Presentation

A man in his early 60s with chronic hepatitis C–induced liver disease presented with a 14-cm right hepatic lobe and biopsy-proven, well-differentiated HCC with a serum alpha fetoprotein (AFP) of 4,092 ng/dL (Figure 1). Additional comorbidities included type 2 diabetes mellitus, obstructive sleep apnea, and poorly controlled chronic hypertension. The patient had preserved liver substrate (Child-Pugh A5, albumin-bilirubin grade 1, platelet count of  $197 \times 10^9/L$ ) and good performance status (Eastern Cooperative Oncology Group 0). Volumetric analysis identified a left hepatic lobe FLR of 15%, which was insufficient for surgical resection. Given the size of the tumor and high AFP, a hepatobiliary multidisciplinary tumor board recommended tumor treatment with neoadjuvant nivolumab and radiation lobectomy with Y-90 (TheraSphere, Boston Scientific Corporation), followed by right hepatectomy if a favorable biologic test of time and adequate FLR hypertrophy were achieved.

### Mapping Angiography

Angiography demonstrated a hyperenhancing right hepatic lobe tumor (Figure 2) supplied predominantly by the right hepatic artery with parasitized contribution from the right 11th intercostal artery and right middle adrenal artery. Technetium-99m–labeled macroaggregated albumin (99m-Tc MAA) 4 mCi was injected via the right hepatic artery, with a calculated lung shunt fraction of 64.3% (Figure 3). The patient's case was re-presented at the hepatobiliary multidisciplinary tumor board and, given the high lung shunt fraction, the decision was made to proceed with PVE instead.

### PVE

Portal venous access was established percutaneously via a trans-splenic approach. Multiple segmental branches of the right portal vein were selected with a microcatheter and embolized with a 10:1 suspension of N-butyl cyanoacrylate and Lipiodol (Guerbet LLC). A postembolization venogram confirmed cessation of blood flow into the right portal vein (Figure 4).

### Postprocedural Events

On arrival to the recovery suite, the patient developed abdominal pain with an associated hypertensive emergency (systolic blood pressure > 200 mm Hg) and was subsequently treated with intravenous antihypertensives. Approximately 1 hour postprocedure,

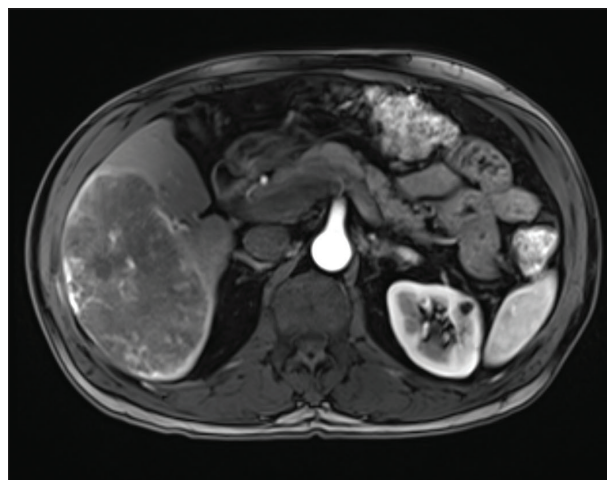


**Figure 1.** Pretreatment axial contrast-enhanced MRI demonstrates a 14-cm, heterogeneously enhancing, well-circumscribed mass in the right hepatic lobe consistent with biopsy-proven HCC.



**Figure 2.** Mapping angiography reveals a right hepatic lobe mass with primarily right hepatic artery blood supply.

the patient experienced severe chest pain followed by pallor, diaphoresis, and hypotension. The patient was transferred to the emergency department, where a contrast-enhanced CT of the chest, abdomen, and pelvis revealed an acute type A aortic dissection with hemopericardium (Figure 5).

After consultation with cardiothoracic surgery, the patient elected to forego emergent surgical repair of his ascending aortic dissection due to his coexisting cancer diagnosis. He was admitted for medical management, stabilized, and discharged to home hospice 6 days after PVE.

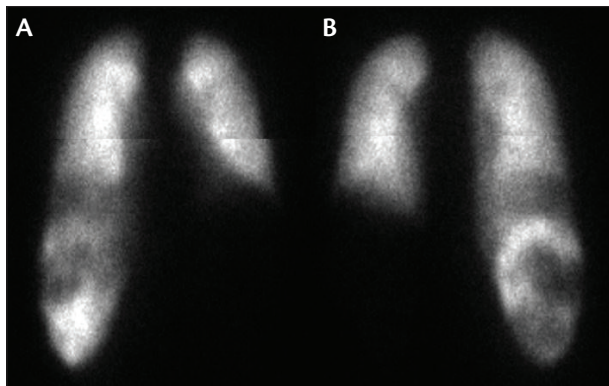


Figure 3. Anterior (A) and posterior (B) planar scintigraphy after  $^{99m}\text{Tc}$  MAA administration shows diffuse radiotracer activity throughout the right hepatic lobe and both lungs. The lung shunt fraction was 64.3%.

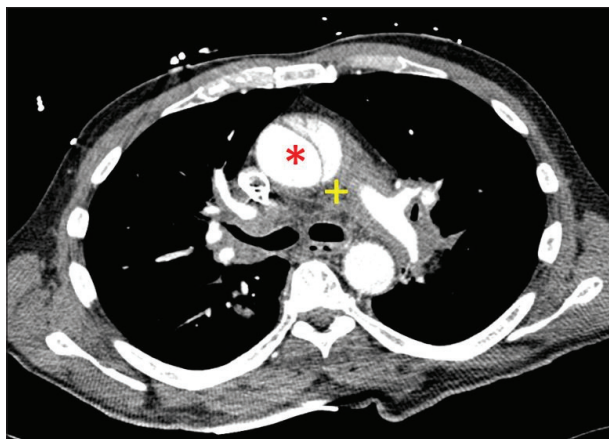


Figure 5. Axial image from the chest CTA reveals an aortic dissection in the ascending aorta (\*) with a pericardial hematoma (+).

Surveillance imaging at 3 months demonstrated continued increase in size of the dissecting thoracic aortic aneurysm and, unexpectedly, a reduction of the right hepatic lobe tumor to 8.7 cm and normalization of serum AFP to 2.9 ng/dL. Given the positive tumor response, the patient elected to proceed with surgical repair of his ascending aorta, which was successfully performed 4 months after PVE.

### HCC Follow-Up

Immunotherapy was reinitiated 1 month after cardiothoracic surgery and subsequently discontinued 5 months later for suspected immune-related scleritis. The patient was followed with serial abdominal imaging and laboratory surveillance every 3 months postthoracotomy. At last follow-up, 24 months after PVE, the right

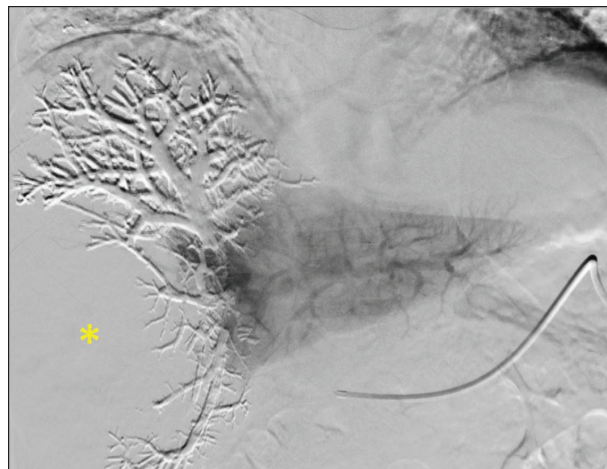


Figure 4. A postembolization venogram demonstrates a photopenic defect in the right hepatic lobe corresponding to tumor (\*) with cessation of flow into the right portal vein and preserved flow into the left portal vein.

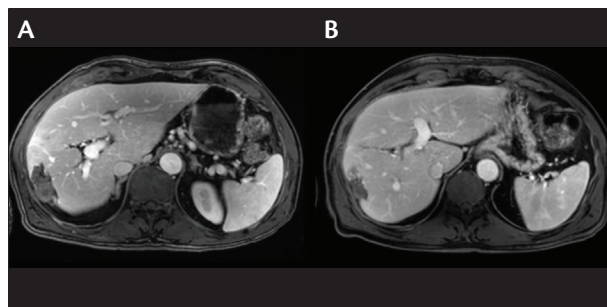


Figure 6. Contrast-enhanced MRI at 6 (A) and 24 (B) months after PVE demonstrates involution of the right hepatic lobe and marked compensatory hypertrophy of the left hepatic lobe without viable tumor.

hepatic lobe tumor demonstrated a complete response as measured by modified Response Evaluation Criteria in Solid Tumors (mRECIST)<sup>5</sup> with a corresponding serum AFP of 2.8 ng/dL (Figure 6). Tumor resection continues to be deferred due to the lack of viable disease per imaging and a normal serum AFP level.

### DISCUSSION

PVE is a safe procedure that has a reported major complication rate of < 1%, although minor adverse events are common, including abdominal pain in 22.9% of patients.<sup>6</sup> Pain management is an important aspect of the postintervention period and is influenced by periprocedural medications and patient risk factors.<sup>7</sup> In patients with cirrhosis, acetaminophen is considered a safe analgesic, while patients with mild chronic liver dis-



ease may tolerate reduced doses of nonsteroidal anti-inflammatory drugs or opioids.<sup>8</sup>

Complete pathologic necrosis has been reported after PVE monotherapy in HCC, with a higher incidence when performed in combination with chemoembolization.<sup>9</sup> Although arterial embolization was not performed in this patient, profound postprocedural hypotension due to the aortic dissection may conceptually have led to added tumor infarction. Furthermore, the concurrent immunotherapy could conceptually have been augmented secondary to antigen release after tumor infarction.<sup>10</sup>

In summary, this case illustrates an unusual complication after PVE resulting in acute type A aortic dissection and complete radiologic response of a 14-cm HCC with a sustained AFP normalization.

1. Marrero JA, Kulik LM, Sirlin CB, et al. Diagnosis, staging, and management of hepatocellular carcinoma: 2018 practice guidance by the American Association for the Study of Liver Diseases. *Hepatology*. 2018;68:723-750. doi: 10.1002/hep.29913
2. Bekki Y, Marti J, Toshima T, et al. A comparative study of portal vein embolization versus radiation lobectomy with yttrium-90 microspheres in preparation for liver resection for initially unresectable hepatocellular carcinoma. *Surgery*. 2021;169:1044-1051. doi: 10.1016/j.surg.2020.12.012
3. Lewandowski RJ, Donahue L, Chocheanachaisakul A, et al. (90)Y radiation lobectomy: outcomes following surgical resection in patients with hepatic tumors and small future liver remnant volumes. *J Surg Oncol*. 2016;114:99-105. doi: 10.1002/jso.24269
4. Ahmed A, Stauffer JA, LeGout JD, et al. The use of neoadjuvant lobar radioembolization prior to major hepatic resection for malignancy results in a low rate of post-hepatectomy liver failure. *J Gastrointest Oncol*. 2021;12:751-761. doi: 10.21037/jgo-20-507
5. Lencioni R, Llovet J. Modified RECIST (mRECIST) assessment for hepatocellular carcinoma. *Semin Liver Dis*. 2010;30:52-60. doi: 10.1055/s-0030-1247132
6. van Lienden KP, van den Esschert JW, de Graaf W, et al. Portal vein embolization before liver resection: a systematic review. *Cardiovasc Intervent Radiol*. 2013;36:25-34. doi: 10.1007/s00270-012-0440-y
7. Hatsipoulou O, Cohen RI, Lang E V. Postprocedure pain management of interventional radiology patients. *J Vasc Interv Radiol*. 2003;14:1373-1385. doi: 10.1097/01.rvi.0000085769.63355.24
8. Chandok N, Watt KDS. Pain management in the cirrhotic patient: the clinical challenge. *Mayo Clin Proc*. 2010;85:451-458. doi: 10.4065/mcp.2009.0534

9. Beppu T, Yamamura K, Okabe H, et al. Oncological benefits of portal vein embolization for patients with hepatocellular carcinoma. *Ann Gastroenterol Surg*. 2021;5:287-295. doi: 10.1002/ags3.12414
10. Murciano-Goroff YR, Warner AB, Wolchok JD. The future of cancer immunotherapy: microenvironment-targeting combinations. *Cell Res*. 2020;30:507-519. doi: 10.1038/s41422-020-0337-2

### Cynthia De la Garza-Ramos, MD

Postdoctorate Research Fellow  
Department of Radiology  
Mayo Clinic  
Jacksonville, Florida  
delagarza-ramos.cynthia@mayo.edu  
*Disclosures: None.*

### Beau B. Toskich, MD

Director of Interventional Oncology  
Division of Interventional Radiology  
Mayo Clinic  
Jacksonville, Florida  
toskich.beau@mayo.edu  
*Disclosures: Advisor to Boston Scientific Corporation and Sirtex Medical.*

### Andrew R. Lewis, MD

Assistant Professor of Radiology  
Division of Interventional Radiology  
Mayo Clinic  
Jacksonville, Florida  
lewis.andrew1@mayo.edu  
*Disclosures: None.*

## Rendezvous Technique for Treatment of Ablation-Related Bile Duct Injury

By Shimwoo Lee, MD; Alireza Sedarat, MD; and Justin P. McWilliams, MD, FSIR

### CASE STUDY

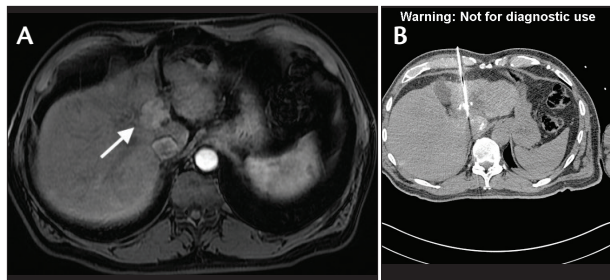
#### Initial Presentation

A man in his mid 60s presented with a history of Child-Pugh class A cirrhosis secondary to hepatitis C complicated by HCC. He underwent transarterial chemoembolization (TACE) of a dominant segment 4 tumor with partial mRECIST response. This was followed by percutaneous microwave ablation using two probes (Neuwave PR-20, Johnson & Johnson) with complete mRECIST response on subsequent imaging (Figure 1). The patient did well perioperatively but had gradually increasing asymptomatic right-sided biliary dilation noted on follow-up MRIs. Five months after the ablation, the patient presented with pruritus, a total bilirubin level of 13.6 mg/dL, and an alka-

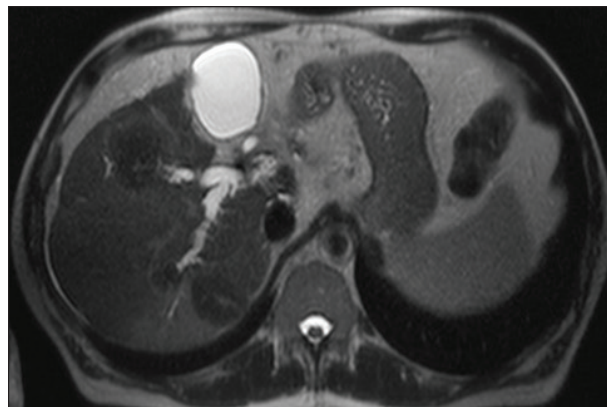
line phosphatase level of 516 U/dL, with right intrahepatic biliary dilatation on MRI (Figure 2). Endoscopic retrograde cholangiopancreatography (ERCP) demonstrated a high-grade stricture at the right hepatic duct centrally and passage of contrast into the segment 4 ablation cavity (Figure 3). The findings were consistent with ablation-related bile duct damage and biloma formation. As the stricture could not be cannulated by ERCP, interventional radiology was consulted for internal-external biliary drain placement to relieve biliary obstruction.

#### Interventions

A right-sided percutaneous transhepatic cholangiogram demonstrated right hepatic biliary ductal dilata-



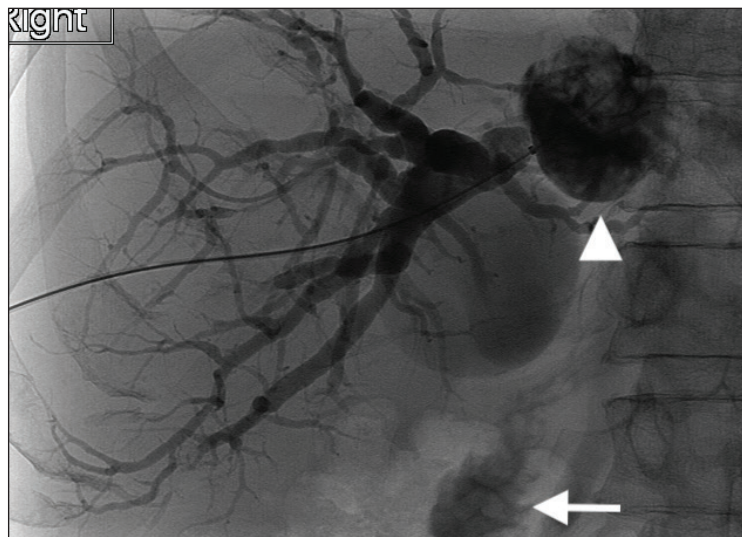
**Figure 1.** Pretreatment MRI abdomen shows cirrhotic liver morphology and an arterially enhancing segment 4 lesion measuring 3.2 cm (arrow) with venous washout (not shown), consistent with HCC (A). Intraprocedural CT image during microwave ablation confirms probe placement within the tumor (B).



**Figure 2.** Follow-up MRI 5 months after ablation shows right intrahepatic biliary dilatation.



**Figure 3.** ERCP demonstrates a high-grade stricture at the right posterior hepatic duct origin and hilum (arrow) as well as a segment 4B postablation cavity (arrowhead), consistent with heat-induced bile duct injury.

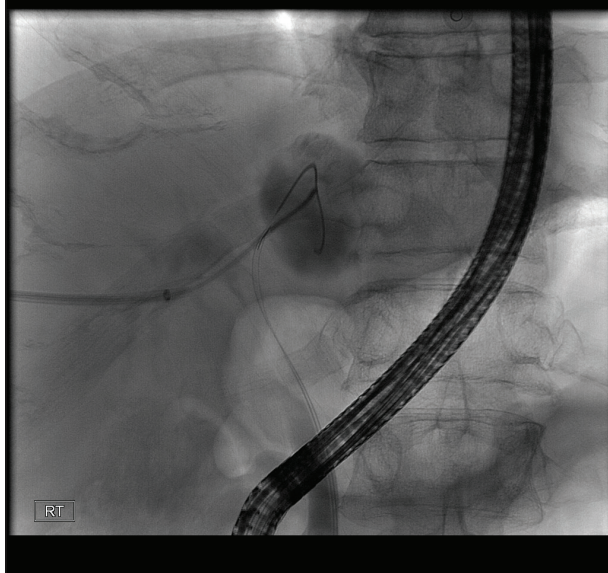


**Figure 4.** Percutaneous transhepatic cholangiogram demonstrates right hepatic biliary ductal dilatation with contrast extending into the segment 4B biloma (arrowhead) with minimal passage into the common bile duct and the small bowel (arrow).

tion with contrast extending into the segment 4 biloma, with minimal passage of contrast into the common duct (Figure 4). Multiple attempts to access the common duct from the right-sided access and through the biloma were unsuccessful. Therefore, an 8-F external right hepatic biliary drain was placed.

Over the next few days, the patient had high-output biliary drainage with persistent hyponatremia resulting from biliary fluid losses, prompting a second attempt to cross into the common duct, which was again unsuccessful. A same-day rendezvous procedure was arranged jointly with interventional radiology and gastroenterol-

ogy. The indwelling biliary drain was exchanged over a wire for a sheath, through which contrast injection was performed. The gastroenterologist cannulated the common duct endoscopically and used a 0.035-inch, 400-cm Jagwire (Boston Scientific Corporation) to pass into the biloma in a retrograde fashion. From the percutaneous right-sided biliary access, the interventional radiologist used a 5-F Kumpe catheter (Cook Medical) and 0.035-inch angled Glidewire (Terumo Interventional Systems) to access the biloma and then placed a 10-mm gooseneck snare, which was used to capture the Jagwire passed from below (Figure 5). The Jagwire was

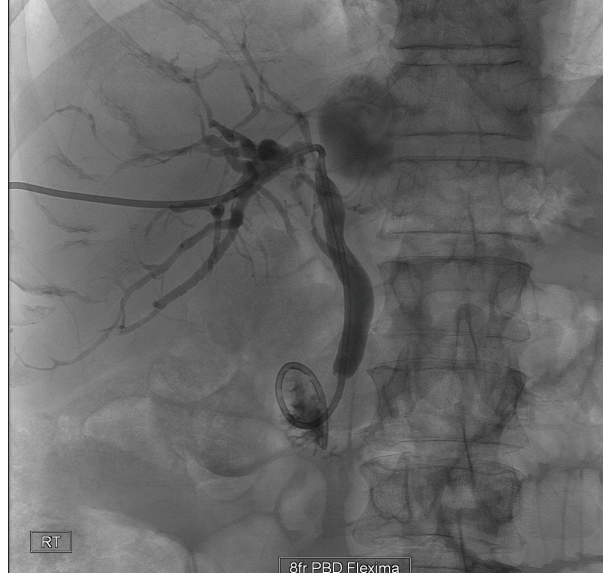
**Warning: Not for diagnostic use**

**Figure 5.** A fluoroscopic image illustrates the rendezvous technique. Endoscopically, a wire was passed through the common bile duct into the biloma in a retrograde fashion. From the percutaneous biliary access, a 10-mm gooseneck snare was passed through a catheter and used to capture the wire.

snared out of the right-sided biliary sheath to achieve through-and-through access, and an 8-F internal-external biliary drain was placed, allowing biliary drainage into the duodenum (Figure 6).

The drain was capped for 6 weeks without complications. A second rendezvous procedure was performed with gastroenterology to internalize the biliary drainage. The indwelling biliary drain was exchanged over a 0.035-inch, 400-cm Jagwire for an 8-F vascular sheath, with the Jagwire tip looped in the small bowel. The wire was snared by the endoscope, facilitating retrograde access into the biliary system and balloon dilation of the biliary stenosis in the right hepatic duct. Three plastic internal biliary stents (two 8 F and one 7 F) were placed in parallel, demonstrating adequate biliary drainage.

The patient subsequently has undergone routine internal biliary stent exchanges every 3 to 4 months by gastroenterology without complications. Two additional ablation procedures have been performed for HCC progression at other sites. Follow-up ERCP demonstrated improvement of the biliary stenosis and resolution of the biloma (Figure 7). More than a year after the initial internal biliary stent placement, the patient has complete response with normal liver function tests and remains on the list for liver transplant.

**Warning: Not for diagnostic use**

**Figure 6.** Cholangiogram shows successful placement of an internal-external biliary drainage catheter using the rendezvous technique.

## DISCUSSION

The incidence of bile duct injury and biloma after percutaneous thermal ablation of the liver is rare. In a cohort of 1,136 patients who underwent microwave ablations of the liver, Liang et al found two patients with biliary complications (0.2%), both of whom had large HCCs in the hepatic hilum.<sup>1</sup> Although bile ducts near the hilum may be partially protected from thermal injury by the heat-sink effect of the adjacent portal vein, disease processes that reduce portal venous flow, such as cirrhosis or portal vein thrombosis, can increase the risk of bile duct injury.<sup>2</sup> Achieving complete treatment of tumors near the hilum without harming the central biliary and portal venous structures is challenging and may not be feasible. Thermal injury of the bile ducts most commonly causes biliary stricture, resulting in biliary obstruction.<sup>2</sup> Clinical manifestations include jaundice, pruritus, and, in severe cases, cholangitis and hepatic abscesses. These tend to occur in the postprocedural period rather than immediately.<sup>1</sup>

Both ERCP and percutaneous transhepatic biliary drainage (PTBD) are potential diagnostic and therapeutic options for bile duct strictures. ERCP with endoscopic biliary drainage is the preferred first choice since the drainage is formed internally from the biliary



**Warning: Not for diagnostic use**

**Figure 7.** Follow-up ERCP 9 months after rendezvous procedure shows improvement of the biliary stenosis and resolution of the biloma.

system into the duodenum.<sup>3</sup> In contrast, PTBD requires creation of a parenchymal tract with external catheters, which is uncomfortable for patients and can dislodge. Moreover, external biliary drainage can lead to excessive loss of bicarbonate-rich bile, with resultant electrolyte abnormalities and orthostatic hypotension. Therefore, PTBD is reserved for patients in whom internal biliary access with ERCP cannot be achieved. A number of factors may preclude an ERCP, including postsurgical anatomy (eg, Roux-en-Y, hepaticojejunostomy), papillary distortion from tumor, duodenal obstruction, and duodenal diverticulum. Both PTBD and ERCP pose a risk of bleeding, biliary sepsis, and cholecystitis.<sup>4</sup>

When neither percutaneous transhepatic or endoscopic retrograde cholangiography alone is sufficient to facilitate biliary-duodenal drainage catheter placement, a rendezvous procedure can be performed. In general, the rendezvous technique aims to reach one point in the body via two access points. Multiple authors have described techniques combining ERCP and PTBD, similar to our case. For instance, Shin et al described placement of a guidewire through the common bile duct and into a biloma by ERCP and subsequent ensnarement from percutaneous transhepatic biliary access to allow placement of an internal-external biliary drainage catheter in a case of surgical common bile duct transection.<sup>5</sup> De Robertis et al also described a totally percuta-

neous rendezvous technique without endoscopy, where bilateral catheterization of bile ducts was performed to treat a type IV biliary stenosis secondary to a hilar cholangiocarcinoma as an alternative to invasive surgery.<sup>6</sup>

In conclusion, a combined rendezvous technique can be used to treat challenging cases of iatrogenic biliary injury when endoscopic or percutaneous biliary access alone fails.

1. Liang P, Wang Y, Yu X, Dong B. Malignant liver tumors: treatment with percutaneous microwave ablation—complications among cohort of 1136 patients. *Radiology*. 2009;251:933-940. doi: 10.1148/radiol.2513081740
2. Kim KR, Thomas S. Complications of image-guided thermal ablation of liver and kidney neoplasms. *Semin Intervent Radiol*. 2014;31:138-148. doi: 10.1055/s-0034-1373789
3. Kapoor BS, Mauri G, Lorenz JM. Management of biliary strictures: state-of-the-art review. *Radiology*. 2018;289:590-603. doi: 10.1148/radiol.2018172424
4. Born P, Rösch T, Brühl K, et al. Long-term outcome in patients with advanced hilar bile duct tumors undergoing palliative endoscopic or percutaneous drainage. *Z Gastroenterol*. 2000;38:483-489. doi: 10.1055/s-2000-14886
5. Shin S, Klevan A, Fernandez CA, et al. Rendezvous technique for the treatment of complete common bile duct transection after multiple hepatobiliary surgeries. *J Laparoendosc Adv Surg Tech A*. 2014;24:728-730. doi: 10.1089/lap.2014.0374
6. De Robertis R, Contro A, Zamboni G, Mansueto G. Totally percutaneous rendezvous techniques for the treatment of bile strictures and leakages. *J Vasc Interv Radiol*. 2014;25:650-654. doi: 10.1016/j.jvir.2013.12.584

### Shimwoo Lee, MD

Division of Interventional Radiology  
Department of Radiology  
UCLA Medical Center  
David Geffen School of Medicine at UCLA  
Los Angeles, California

*Disclosures: None.*

### Alireza Sedarat, MD

Division of Digestive Diseases  
UCLA Medical Center  
David Geffen School of Medicine at UCLA  
Los Angeles, California

*Disclosures: None.*

### Justin P. McWilliams, MD, FSIR

Division of Interventional Radiology  
Department of Radiology  
UCLA Medical Center  
David Geffen School of Medicine at UCLA  
Los Angeles, California  
jumcwilliams@mednet.ucla.edu

*Disclosures: Consultant to Johnson & Johnson, Asahi Intecc, Terumo, Siemens, and Penumbra.*

# Treatment of Bronchopleural Fistula After Thoracic Cryoablation

By David Zucker, MD, and Scott Genshaft, MD

## CASE STUDY

### Initial Presentation and Procedure

A woman in her early 60s with a history of colorectal cancer with metastases to liver and lung and multiple rounds of chemotherapy, thoracic radiation, partial hepatectomy, and cryoablation of a left lower lobe metastasis presented for additional locoregional therapy of enlarging pulmonary metastases. The patient was placed in the prone position on the CT procedure table. Under moderate sedation, three Perc-24 probes and one Perc-17 probe (Endocare) were placed with CT guidance in a 4.7- X 3.3-cm lesion in the medial basal segment of the left lower lobe (Figure 1). Cryoablation was chosen per operator preference due to intraprocedural visualization of ice formation and decreased risk of pleural injury given the juxtapleural location of the target lesion. Ablation was performed per modified triple-freeze technique.<sup>1</sup> The probes were then withdrawn 2 cm, and an additional 8-minute freeze and 2-minute active thaw were performed prior to needle removal. During ablation, a small pneumothorax developed, and a 14-F J-tip all-purpose drain was placed into the left pleural space via Seldinger technique. The ablation needles were removed with tract cautery, and the patient was placed in the left lateral decubitus position, a standard postprocedural measure

to prevent spread of fluid to the contralateral lung. An additional scan was performed after 10 minutes, which showed a moderate left pleural effusion. The patient was placed in the supine position, the anterior chest was prepared in a sterile fashion, and a 24-F Thal-Quick chest tube (Cook Medical) was placed via Seldinger technique in the left anterior third intercostal space, which immediately yielded 200 mL of serosanguinous pleural fluid (Figure 2). The tube was connected to -20-cm H<sub>2</sub>O wall suction, the previously placed 14-F drain was removed, and a petroleum jelly gauze dressing was applied. Portable chest radiographs were obtained 1 and 3 hours postprocedure per operator protocol, and the patient was admitted for overnight observation. The patient was discharged home in stable condition on postprocedure day 1 with the pleural catheter connected to a Heimlich valve and drainage bag.

### Interventions

The patient's chest tube was removed in the outpatient clinic setting 5 days postablation. The patient presented to the emergency department 11 days postablation for shortness of breath. Chest radiograph at that time demonstrated a large left hydropneumothorax without mediastinal shift (Figure 3). An 18-F Thal-Quick

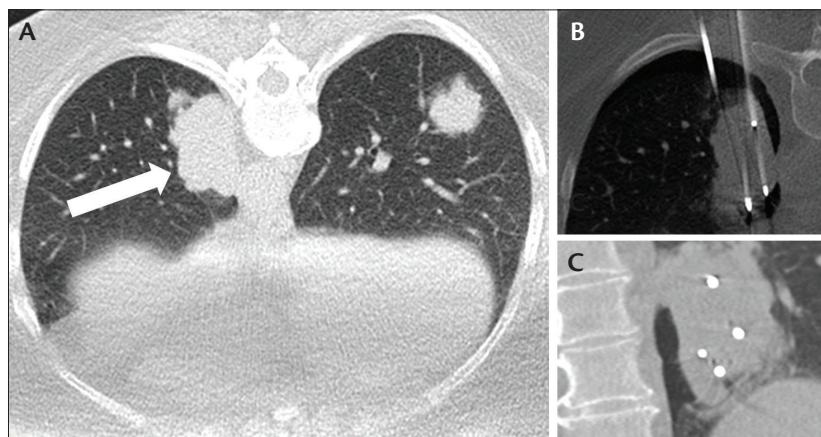


Figure 1. Preprocedural noncontrast axial CT image of the lower thorax shows a lobulated mass in the medial basal segment of the left lower lobe measuring up to 4.7 cm abutting the pleura (arrow) (A). Representative axial image during needle placement. A small pneumothorax is present (B). Coronal reformat during needle placement (C).

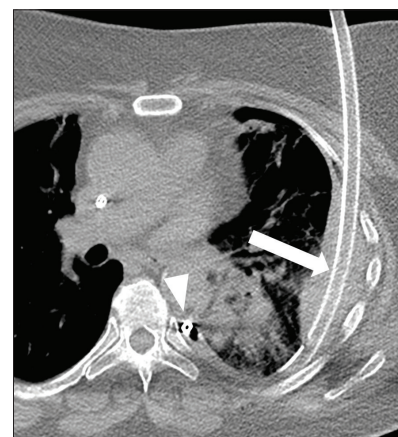


Figure 2. A 24-F chest tube (arrow) placed into a hemopneumothorax. A previously placed 14-F (arrowhead) chest tube was subsequently removed.



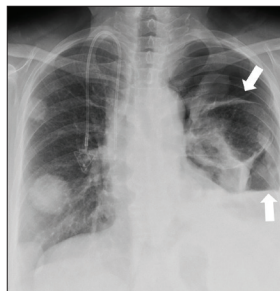


Figure 3. Large left hydro-pneumothorax (arrows).

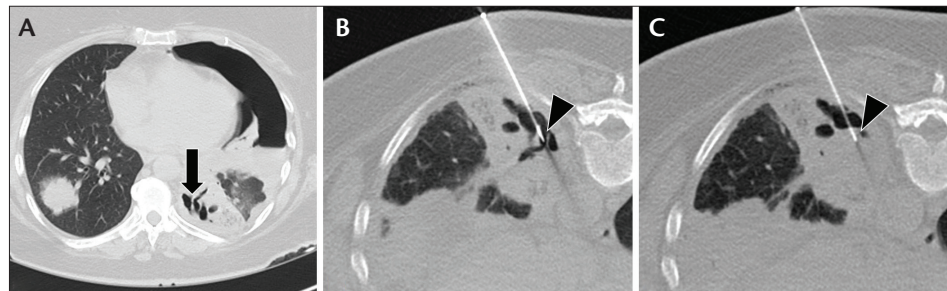


Figure 4. Axial CT image at the level of the prior ablation zone demonstrates communication between the pleural space and cavitary central ablation zone (arrow) (A). A 19-gauge needle was advanced to the BPF (arrowhead) (B). Coseal and autologous blood were delivered through the needle, filling the BPF (arrowhead) (C).

chest tube was placed with CT guidance, and 250 mL of fluid and 100 mL of air were evacuated. CT demonstrated cavitation of the central ablation zone with communication to the pleural space, indicative of bronchopleural fistula (BPF) (Figure 4A).

The patient returned 2 days after chest tube placement for treatment of the BPF. The patient was placed prone on the CT table. With moderate sedation and local anesthesia, a 19-gauge coaxial needle was advanced to the BPF under intermittent CT guidance. Coseal surgical sealant (Baxter) and 30 mL of autologous blood patch were delivered through the coaxial needle, completely filling the cavity (Figure 4B and 4C). No further air leak was detected via the chest tube and water seal device. Follow-up radiographs after placing the chest tube to the water seal and clamping demonstrated no recurrence of the left pneumothorax, and the patient was discharged home on postprocedure day 3.

The patient was followed for another 14 months, during which she was treated with an additional cryoablation procedure for a separate metastasis and with systemic chemotherapy on a clinical trial basis. She had no recurrence of pneumothorax on follow-up imaging, consistent with terminal closure of the prior BPF. The patient died due to cancer-related causes 27 months after BPF treatment.

## DISCUSSION

Although procedure-related pneumothorax is a common, anticipated, and often unpreventable occurrence after thoracic interventions, the incidence of BPF after pulmonary thermal ablation is rare, complicating < 1% of such interventions.<sup>2,3</sup> One large series evaluated 1,000 pulmonary radiofrequency ablation (RFA) procedures in 420 patients at a single institution and demonstrated that 0.4% of their ablation procedures resulted in BPF formation.<sup>2</sup> Although fewer data are available regarding

cryoablation, juxtapleural target location is considered a risk factor for BPF formation after thermal ablation.<sup>2,4</sup> Additional risk factors for BPF include prior radiation therapy, primary pulmonary neoplasm, chronic bronchitis, and emphysema.<sup>4</sup> BPF should be suspected in patients with persistent pneumothorax and evidence of air leak after placement of a chest tube.

In our institution, it is standard practice to obtain portable chest radiographs at 1 and 3 hours postablation. Chest tubes are placed for symptomatic pneumothoraces, as well as for moderate-to-large pneumothoraces and for small pneumothoraces that demonstrate interval expansion. Most uncomplicated pneumothoraces are managed on an outpatient basis with the chest tube connected to a Heimlich valve prior to discharge. Chest tube size of at least 14 F is preferred in our practice, as they facilitate rapid, low-resistance evacuation of air and fluid. All patients are counseled to return to the emergency department if they experience sudden chest pain or difficulty breathing.

Historically, BPFs that fail conservative management with chest tube placement are treated with more invasive procedures, including pleurodesis, endobronchial treatment, and surgical management.<sup>5</sup> In lieu of potentially painful, morbid treatment options, interventionalists at our institution now favor attempted closure with minimally invasive techniques prior to involving additional specialists. Case reports and case series demonstrate feasibility of percutaneous delivery of various sealants to permanently treat BPFs.<sup>6,7</sup> A series of six procedures using Coseal in five patients at our institution resulted in effective treatment of four out of five patients; one patient had persistent air leak and went on to have further treatment with placement of endobronchial valves.<sup>6</sup> An autologous blood patch was used in two cases.

The authors believe that interventionalists should address their own complications whenever possible.

An approach to safely and effectively address postablation BPF allows the interventionalist to provide more complete care for the patient and may spare further morbidity and expense incurred in pursuing further treatment. Coseal is a bioabsorbable polymer that can be delivered via a coaxial needle and expands to 400% of its initial volume over 24 hours and is indicated for adjunctive hemostasis vascular reconstructions.<sup>8</sup> Autologous blood patch has long been used to treat persistent air leak via pleurodesis, although its use for treatment of BPF by targeted delivery has not been widely reported.<sup>9,10</sup> The use of autologous blood, Coseal polymer, or combination therapy allows for safe, expeditious, targeted treatment of this rare but feared complication.

1. Pan PJ, Bansal AK, Genshaft SJ, et al. Comparison of double-freeze versus modified triple-freeze pulmonary cryoablation and hemorrhage volume using different probe sizes in an in vivo porcine lung. *J Vasc Interv Radiol*. 2018;29:722-728. doi: 10.1016/j.jvir.2017.11.016
2. Kashima M, Yamakado K, Takaki H, et al. Complications after 1000 lung radiofrequency ablation sessions in 420 patients: a single center's experiences. *Am J Roentgenol*. 2011;197:W576-W580. doi: 10.2214/AJR.11.6408
3. Sakurai J, Hiraki T, Mukai T, et al. Intractable pneumothorax due to bronchopleural fistula after radiofrequency ablation of lung tumors. *J Vasc Interv Radiol*. 2007;18:141-145. doi: 10.1016/j.jvir.2006.10.011
4. Alberti N, Buy X, Frulio N, et al. Rare complications after lung percutaneous radiofrequency ablation: incidence, risk factors, prevention and management. *Eur J Radiol*. 2016;85:1181-1191. doi: 10.1016/j.ejrad.2016.03.032
5. Sakata KK, Reissenauer JS, Kern RM, Mullon JJ. Persistent air leak—review. *Respir Med*. 2018;137:213-218. doi: 10.1016/j.rmed.2018.03.017
6. Shahrouki P, Barclay J, Khan S, et al. Treatment of post-ablation bronchopleural fistula using percutaneous synthetic hydrogel surgical sealant: initial experience of safety and efficacy. *Cardiovasc Interv Radiol*. 2021;44:325-332. doi: 10.1007/s00270-020-02691-3
7. Powell DK, Baum S. Bronchopleural fistula treated with N-butyl cyanoacrylate glue after ablation. *J Vasc Interv Radiol*. 2018;29:1692-1693. doi: 10.1016/j.jvir.2018.06.008

Radiol. 2018;29:1692-1693. doi: 10.1016/j.jvir.2018.06.008

8. COSEAL surgical sealant. Accessed July 26, 2021. <https://advancedsurgery.baxter.com/products/coseal>

9. Clark JM, Cooke DT, Brown LM. Management of complications after lung resection: prolonged air leak and bronchopleural fistula. *Thorac Surg Clin*. 2020;30:347-358. doi: 10.1016/j.thorsurg.2020.04.008

10. Dugan KC, Laxmanan B, Murgu S, Hogarth DK. Management of persistent air leaks. *Chest*. 2017;152:417-423. doi: 10.1016/j.chest.2017.02.020

### David Zucker, MD

Division of Interventional Radiology  
Department of Radiology  
UCLA Medical Center  
David Geffen School of Medicine at UCLA  
Los Angeles, California  
*Disclosures: None.*

### Scott Genshaft, MD

Division of Interventional Radiology  
Department of Radiology  
UCLA Medical Center  
David Geffen School of Medicine at UCLA  
Los Angeles, California  
[sgenshaft@mednet.ucla.edu](mailto:sgenshaft@mednet.ucla.edu)  
*Disclosures: Consultant to Boston Scientific Corporation and Medtronic.*

## Hemorrhage After Renal Ablation

By Nora Tabori, MD, and Eric You, MD

### CASE STUDY

A man in his late 60s underwent routine workup for renal insufficiency, and an ultrasound revealed a right renal mass. CT and MRI were performed, revealing an exophytic cystic and solid mass from the right kidney (Figure 1). The patient was sent to urology for possible surgical resection. Although the mass was potentially resectable, the patient had other comorbidities that made a surgical approach risky, including morbid obesity, diabetes mellitus, hypertension, hyperlipidemia, and prior weight loss surgery. Ultimately, it was decided to have the mass ablated percutaneously, also with the assistance of anesthesia.

### PROCEDURAL OVERVIEW

The patient underwent routine outpatient cryoablation using five probes and freeze/thaw cycles. Postablation scans showed no immediate complication. Recovery was unremarkable, and the patient was discharged home.

En route to home, the patient had sudden pain and dizziness, and presented to the nearest emergency department. At the outside hospital, a diagnostic CT scan revealed a perinephric hematoma (Figure 2); the patient was hemodynamically stable but his hemoglobin had dropped 3 g/dL. The patient was subsequently transferred back to the original hospital where cryoablation had been performed.

On arrival, the patient was taken immediately for a diagnostic angiogram; no active bleeding pseudoaneurysm could be identified (Figure 3). The patient was discharged home after 48 hours of observation. Only 1 unit of packed red blood cells were required during the hospitalization, and the patient remained hemodynamically stable.

### DISCUSSION

Percutaneous ablation of renal masses is a minimally invasive procedure that can help patients who do not desire or cannot have surgical resection. In a meta-analysis

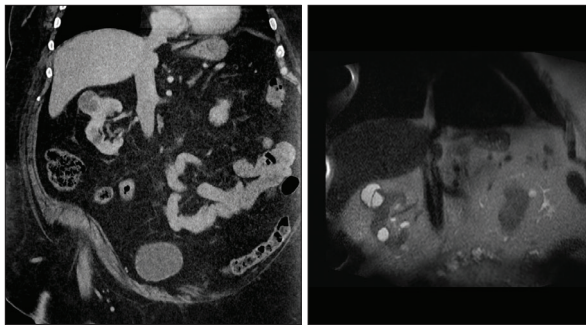


**Figure 1.** Diagnostic CT and MRI shows exophytic solid and cystic mass.



**Figure 2.** CT scan shows post-ablation perinephric hematoma.



**Figure 3.** Diagnostic angiogram of the kidney. No active bleeding was identified.

sis, percutaneous ablations had lower efficacy compared to surgery (87% vs 97%) but also decreased complication rates (7% vs 3%). Some of the major complications for the percutaneous approach from this series included hematuria with significant blood clots resulting in urinary obstruction, significant blood loss, urothelial injury, bowel injury, and tract seeding. Minor complications included infection, perirenal hematoma, transient hematuria, and transient neuropathy. Average length of stay was significantly shorter for the percutaneous approach ( $1.4 \pm 0.6$  days) as compared with the surgical approach ( $3.0 \pm 1.3$  days).<sup>1</sup>

Percutaneous ablation complications including hemorrhage and renovascular injury were more commonly seen in renal cryoablation compared to RFA in one series (4.8% vs 1.2%). Hemorrhage was more often seen in cryoablation when compared to RFA, likely from cauterization when using heat-based methods. Some risk factors included location of tumor, with central tumors having more complications, and number of probes.<sup>2</sup>

In our institution, we have considered the utility of preablation embolization. Renal cell carcinoma is notorious for its hypervascular supply, and we often provide preoperative embolization for surgical resection for renal cell carcinoma metastatic disease. However, a propensity score–matched study comparing percutaneous cryoablation alone to percutaneous cryoablation plus transarterial embolization (TAE) demonstrated no objective benefits.<sup>3</sup> Given the lack of data, the additional risks incurred, and the burden placed on the patient and system, we have not chosen to incorporate this practice. In this case patient, one factor we identified that may have helped was to place the patient into overnight observation because of his long commute. Although it may have not prevented the complication, the outcome could have been potentially worse given his remote location.

Percutaneous ablation is a viable alternative to surgical resection for renal masses. Although the percutaneous approach is minimally invasive with lower risk and provides excellent efficacy, complications can occur, and admitting patients for observation should be strongly considered if there are any elevated risk factors, including remote location from the hospital.

1. Hui GC, Tuncali K, Tatli S, et al. Comparison of percutaneous and surgical approaches to renal tumor ablation: metaanalysis of effectiveness and complication rates. *J Vasc Interv Radiol.* 2008;19:1311–1320. doi: 10.1016/j.jvir.2008.05.014

2. Atwell TD, Carter RE, Schmit GD, et al. Complications following 573 percutaneous renal radiofrequency and cryoablation procedures. *J Vasc Interv Radiol.* 2012;23:48–54. doi: 10.1016/j.jvir.2011.09.008

3. Gunn AJ, Mullenbach BJ, Poundstone MM, et al. Transarterial embolization of renal cell carcinoma as an adjunctive therapy prior to cryoablation: a propensity score matching analysis. *Diagn Interv Radiol.* 2018;24:357–363. doi: 10.5152/diir.2018.18090

### Nora Tabori, MD

Associate Professor of Radiology  
MedStar Georgetown University Hospital  
Chief of Interventional Radiology  
MedStar Washington Hospital Center  
Washington, DC  
nora.e.tabori@medstar.net

*Disclosures: Speaker and advisory board member for Boston Scientific.*

### Eric You, MD

Interventional Radiology Fellow  
MedStar Georgetown University Hospital  
Washington, DC

*Disclosures: None.*



## Overcoming Biopsy Complications in Treating HCC

By Arthie Jeyakumar, MD, and Guy E. Johnson, MD

### CASE STUDY

#### Initial Presentation

A 66-year-old man with well-compensated Child-Pugh A hepatitis C cirrhosis was found to have a mass in segment 7 on screening ultrasound. A multiphase CT scan demonstrated an arterially enhancing mass measuring 5.6 cm with delayed phase washout, consistent with a Liver Imaging Reporting and Data System (LI-RADS) 5 lesion, definitely HCC (Figure 1). The AFP was 10,900 µg/L. A biopsy was subsequently performed at an outside hospital, and pathology confirmed the diagnosis of HCC. The patient was discussed in our multidisciplinary liver tumor board with a consensus treatment plan of Y-90 selective radioembolization (radiation segmentectomy). Preprocedural laboratory results included a platelet count of  $97 \times 10^3/\mu\text{L}$ , international normalized ratio of 1.2, albumin of 3.7 g/dL, and total bilirubin of 1.4 mg/dL.

#### Procedure

A mapping angiogram was obtained, which demonstrated an unexpected arteriportal fistula (APF) at the right lateral margin of the tumor between the segment 7 artery and the right posterior portal division. Adjacent to this APF was a presumed iatrogenic pseudoaneurysm (Figure 2), which had formed within the tumor related to the prior biopsy; this was not present on the diagnostic CT or ultrasound (Figure 3). Due to the presence of both the APF and intratumoral pseudoaneurysm, the patient was

rediscussed at tumor board, and the plan was switched to bland TAE and drug-eluting bead TACE (DEB-TACE).

Using a 2.8-F microcatheter, the segment 7 artery was selectively catheterized and again showed the APF. The microcatheter was advanced distal to the APF within the segmental artery, and from this location, doxorubicin-eluting beads (100–300-µm beads) were infused. The catheter was then pulled back proximal to the fistula and an additional 300–500-µm microspheres were infused. Angiography showed persistent filling of both the APF and pseudoaneurysm; therefore, larger 500–700-µm microsphere particles were infused from the same location in an effort to exclude perfusion of the pseudoaneurysm. Additional DEB-TACE was carried out from the proximal segment 7 artery while minimizing portal embolization. The final angiogram demonstrated occlusion of the presumed iatrogenic APF and intratumoral pseudoaneurysm (Figure 4). The patient tolerated the procedure well with no immediate or delayed postprocedural complications. Follow-up imaging demonstrated concern for viable tumor in the segment 7–treated tumor as well as two adjacent lesions that had demonstrated interval growth compatible with LI-RADS 4 lesions. The patient subsequently underwent selective Y-90 radioembolization targeting segment 7 using a radiation segmentectomy approach. The mapping angiogram prior to this procedure demonstrated no perfusion of the pseudoaneurysm or arteriportal shunt (APS).

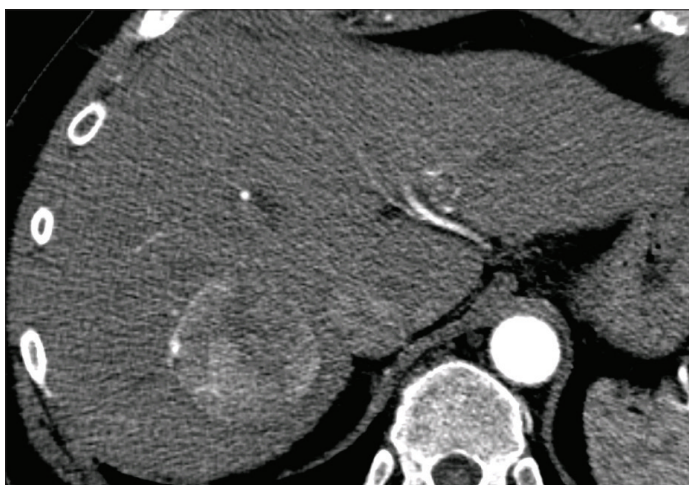
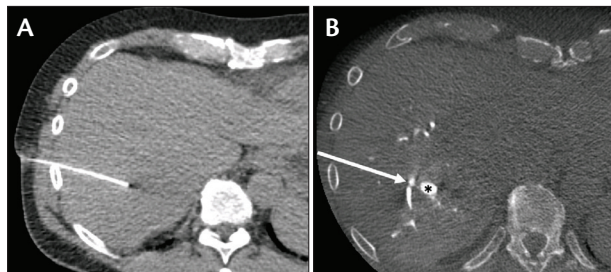


Figure 1. Multiphase CT of the liver shows an arterially enhancing mass in segment 7. The mass demonstrated delayed phase washout (not shown), consistent with HCC.



Figure 2. Y-90 mapping arteriogram. Segment 7 hepatic arteriogram demonstrates an APS with opacification of portal vein branches (arrows) as well as a pseudoaneurysm within the HCC (asterisk).



**Figure 3.** CT axial image demonstrates the trajectory of the core biopsy performed at the outside hospital (A). C-arm CT image obtained during Y-90 mapping angiogram demonstrates a pseudoaneurysm (asterisk). The trajectory of the needle from the biopsy is shown (white arrow), intersecting the segment 7 artery. In addition to the pseudoaneurysm, biopsy needle puncture of the adjacent portal vein (not shown) was likely the cause of the APF (B).

Follow-up imaging after Y-90 radiation segmentectomy showed a mRECIST complete response (Figure 5).

## DISCUSSION

IO has become instrumental in the localized therapy of malignant tumors and serves as a primary or adjunctive therapy in addition to surgery, radiotherapy, and chemotherapy. The approach to treatment for these malignant tumors, particularly HCC, requires a multidisciplinary team to discuss various pathways. Unlike other malignancies, HCC can be diagnosed with cross-sectional imaging obviating the need for tissue sampling in many cases. LI-RADS was developed for the standardized interpretation, reporting, and data collection of patients at risk for HCC undergoing liver imaging. In the 2018 version of LI-RADS, the category 5 designation has a sensitivity of 53.7% and a specificity of 97.3%.<sup>1-3</sup>

According to the American Association for the Study of Liver Diseases (AASLD), a nodule > 2 cm that displays a typical vascular pattern on contrast-enhanced CT or contrast-enhanced MRI can be considered HCC without biopsy.<sup>4-6</sup> The AASLD recommends tissue diagnosis in cases of atypical radiologic features of suspected lesions.<sup>4-6</sup> Although the complications associated with image-guided liver lesion biopsy are rare, the question of whether biopsy should be performed is an individualized one, taking into account lesion size, cross-sectional visibility, LI-RADs characteristics, and transplant eligibility. Curative treatments such as resection, liver transplantation, and ablation rely on small size and localized extent; therefore, early diagnosis is paramount as tumor staging is the most important predictor of survival in HCC.<sup>7</sup> As a result of ultrasound surveillance programs, smaller lesions are being discovered, which are subject to earlier treatment with positive results.

Nevertheless, the smaller dimensions of lesions detected on screening ultrasound make HCC diagnosis a challenge without histologic confirmation because tiny focal lesions are more likely to be premalignant (dysplastic) or even benign (regenerative) nodules.<sup>8-10</sup> According to AASLD guidelines, approximately 52% to 56% of patients with nodules 10 to 20 mm in size may require biopsy.<sup>4,5,11</sup> Tanaka et al demonstrated that 31 nodules detected by ultrasonography could not be found by CT with histologic diagnosis consistent with HCC in 55% of cases.<sup>12</sup>

HCC is occasionally associated with arteriovenous shunts, which are more commonly arteriportal in nature. Significant APS may be a poor predictor of microsphere localization in HCCs and may have implications on locoregional therapy of the liver, resulting in subtherapeutic tumoricidal dosages with increased morbidity risks.<sup>13</sup> The  $\beta$  radiation from Y-90 penetrates an average of 2.5 mm in tissue; however, nontarget radioembolization may lead to complications such as radioembolization-induced liver disease. Although tumors can be associated with APSs, this particular case was most likely iatrogenic and the result of core needle biopsy during which the needle passed through the artery, portal vein, and tumor. In the future, more biopsies may be performed to help guide targeted therapy for HCC, but these therapeutic options are not yet available outside of clinical trials. Because CT was diagnostic of HCC, no biopsy was necessary to confirm the diagnosis, and the biopsy did not inform any subsequent decision-making.

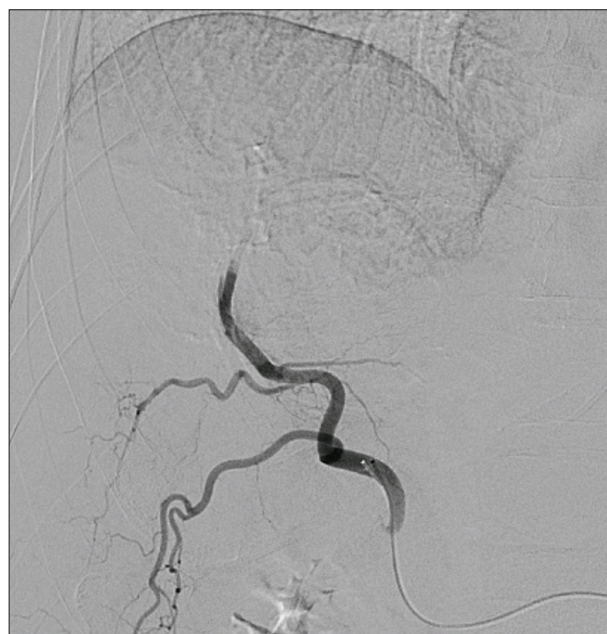


**Figure 4.** Arteriogram after TACE and TAE of the segment 7 hepatic artery demonstrates occlusion of the APF and intratumoral pseudoaneurysm.





**Figure 5.** Multiphase CT of the liver 2 months after Y-90 radiation segmentectomy shows complete response of the segment 7 HCC.

Guiding the initial treatment plan, outcomes from selective Y-90 radioembolization have been shown to be superior to selective TACE in treating HCC.<sup>14</sup> However, concerns were raised about nontarget parenchymal Y-90 and risk of other complications because of the brisk APF and the iatrogenic pseudoaneurysm related to the liver biopsy. Y-90 microspheres measure 20 to 30  $\mu$ m in diameter and therefore are more likely to pass through shunts such as an APF compared to particles used in TACE. Therefore, a change in plan was made in an effort to both treat the iatrogenic APF and the tumor simultaneously. The tumor, fistula, and pseudoaneurysm were treated initially with a combination of TACE and TAE. TACE in patients with large APSs can cause significant PVE, resulting in hepatic ischemia. Although techniques to treat significant APSs by using gelatin sponge or coil embolization have been described, these techniques do not treat the HCC and therefore do not contribute to overall survival.<sup>15,16</sup> Portal vein occlusion of APSs during TACE has demonstrated some promise in overcoming these difficult situations, but data are relatively limited. In our case, this technique was considered; however, TAE/TACE was preferred due to the peripheral location of the tumor, and although it was not the definitive treatment for the tumor, this initial therapy closed the APF and treated the pseudoaneurysm. When residual disease was evident on follow-up imaging, the tumor and small satellite tumors could be definitively treated with curative-intent Y-90 radiation segmentectomy with no treatment-related compromise in liver function.

Progress in recent years, particularly better scanning protocols with CT and MRI and LI-RADS criteria, has

increased the detection rate and diagnostic certainty of HCC. Although often the diagnosis of HCC can be made by imaging alone, with advancements in therapy, histologic assessment may also offer additional information in assessing prognosis and tailoring therapy in the future. As such, although complications associated with liver biopsy are rare, interventional radiologists should be prepared for various techniques to address these sequelae. ■

1. American College of Radiology. Liver Imaging Reporting and Data System (LI-RADS) version 2018. Accessed August 23, 2021. <https://www.acr.org/Clinical-Resources/Reporting-and-Data-Systems/LI-RADS>
2. Elsayes KM, Hooker JC, Agrons MM, et al. 2017 version of LI-RADS for CT and MRI imaging: an update. *Radiographics*. 2017;37:1994-2017. doi: 10.1148/rq.2017170098
3. Alhasan A, Cerny M, Olivieri D, et al. LI-RADS for CT diagnosis of hepatocellular carcinoma: performance of major and ancillary features. *Abdom Radiol*. 2019;44:517-528. doi: 10.1007/s00261-018-1762-2
4. Rockey DC, Caldwell SH, Goodman ZD, et al. Liver biopsy. *Hepatology*. 2009;49:1017-1044. doi: 10.1002/hep.22742
5. Khalifa A, Rockey DC. The utility of liver biopsy in 2020. *Curr Opin Gastroenterol*. 2020;36:184-191. doi: 10.1097/MOG.0000000000000621
6. Neuberger J, Patel J, Caldwell H, et al. Guidelines on the use of liver biopsy in clinical practice from the British Society of Gastroenterology, the Royal College of Radiologists and the Royal College of Pathology. *Gut*. 2020;69:1382-1403. doi: 10.1136/gutjnl-2020-321299
7. Sangiovanni A, Del Ninno E, Fasani P, et al. Increased survival of cirrhotic patients with a hepatocellular carcinoma detected during surveillance. *Gastroenterology*. 2004;126:1005-1014. doi: 10.1053/j.gastro.2003.12.049
8. Kanematsu M, Hoshi H, Yamada T, et al. Small hepatic nodules in cirrhosis: ultrasonographic, CT, and MRI imaging findings. *Abdom Imaging*. 1999;24:47-55. doi: 10.1007/s002619900439
9. Lim JH, Cho JM, Kim EY, et al. Dysplastic nodules in liver cirrhosis: evaluation of hemodynamics with CT during arterial portography and CT hepatic arteriography. *Radiology*. 2000;214:869-874. doi: 10.1148/radiology.214.3.r00mr12869
10. Rode A, Bancel B, Douek P, et al. Small nodule detection in cirrhotic livers: evaluation with US, spiral CT, and MRI and correlation with pathological examination of explanted liver. *J Comput Assist Tomogr*. 2001;25:327-336. doi: 10.1097/00004728-200105000-00001
11. Jain D. Tissue diagnosis of hepatocellular carcinoma. *J Clin Exp Hepatol*. 2014;4(suppl 3):S67-S73. doi: 10.1016/j.jceh.2014.03.047
12. Tanaka Y, Sasaki Y, Katayama K et al. Probability of hepatocellular carcinoma of small hepatocellular nodules undetectable by computed tomography during arterial portography. *Hepatology*. 2000;31:890-898. doi: 10.1053/he.2000.5979
13. Tan AE, Kao YH, Xie W. Excessive hepatic arterial-portal venous shunting may predict failure of microparticle localization in hepatocellular carcinomas. *World J Nucl Med*. 2013;12:48-50. doi: 10.4103/1450-1147.113966
14. Padia SA, Johnson GE, Horton KJ, et al. Segmental yttrium-90 radioembolization versus segmental chemoembolization for localized hepatocellular carcinoma: results of a single-center, retrospective, propensity score-matched study. *J Vasc Interv Radiol*. 2017;28:777-785.e1. doi: 10.1016/j.jvir.2017.02.018
15. Tarazov PG. Intrahepatic arterioportal fistulae: role of transcatheter embolization. *Cardiovasc Intervent Radiol*. 1993;16:368-373.
16. Furuse J, Iwasaki M, Yoshino M, et al. Hepatocellular carcinoma with portal vein tumor thrombus: embolization of arterioportal shunts. *Radiology*. 1997;204:787-790. doi: 10.1148/radiology.204.3.9280260

### Arthie Jeyakumar, MD

Department of Radiology  
Section of Interventional Radiology  
University of Washington  
Seattle, Washington  
*Disclosures: None.*

### Guy E. Johnson, MD

Department of Radiology  
Section of Interventional Radiology  
University of Washington  
Seattle, Washington  
gej@uw.edu  
*Disclosures: Receives consulting fees from Boston Scientific, Genentech, and AstraZeneca.*